ISSN(Online): 2319-8753
ISSN (Print): 2347-6710

International Journal of Innovative Research in Science, Engineering and Technology

(A High Impact Factor, Monthly Peer Reviewed Journal)

Vol. 5, Issue 1, Januray 2016

Superconductivity in Simple Binary Intermetallics

Ramesh Sharma[1] and Yamini Sharma [1, 2*]

Research Scholar, Department of Physics, Mewar University, Chittorgarh-312901 Rajasthan, India[1]

Associate Professor, Dept. of Physics, Feroze Gandhi College, Raebareli-229001 U.P, India[1, 2]

ABSTRACT: Some intermetallic compounds with superconducting properties were investigated by density functional theory. The electronic properties such as energy band structures, density of states, charge density and Fermi surfaces of cubic $ScGa_3$ and $ScIn_3$ were calculated to understand the nature of superconductivity in these intermetallics. The states at Fermi energy level are composed mainly of hybridized 3d-orbitals of Sc and 3p/4p-orbitals of Ga/In and $N(E_F)$ is marginally greater in $ScIn_3$ due to greater weight of Sc d-states. Optical conductivity is found to increase as a result of absorbing photons and falls to low values beyond 11 eV in the UV regions. $ScGa_3$ shows very high conductivity in the visible region and a red shift in the peaks is observed in $ScIn_3$. The temperature dependent properties such as Hall and Seebeck coefficient increase marginally in $ScIn_3$, although thermal conductivity decreases. From the low temperature specific heat, we have estimated the electron-phonon coupling constant $\lambda_{el\text{-}ph}$ which has a value of 0.31 for $ScGa_3$. The vibrational properties illustrate softening of modes in $ScGa_3$ which makes the lattice unstable. The calculated properties confirm that both $ScGa_3$ and $ScIn_3$ are weak intermediate coupling superconductors.

KEYWORDS: Electronic structure, optical, transport properties, phonon dispersion, superconductivity

I. INTRODUCTION

The recent discovery of superconductivity in simple $AuCu_3$ type systems has stimulated much activity in the search for new superconducting materials [1]. Electron spin resonance study of $LaIn_3$ and $LaSn_3$ systems by Bittar et al. showed that these materials behave like conventional superconductors [2]. The pressure dependence of Fermi surface and elastic properties of various AB_3 intermetallics (A=La, Y and X=Sn, Pb, In, Tl) with high superconducting transition temperatures was investigated by FPLAPW methods by Ram et al. [3-5]. The effect of pressure on the Fermi surface topology and cyclotron masses of superconducting rare-earth gallium compound $ErGa_3$ was studied by dHvA effect. The electronic structure was also studied by LMTO-ASA (linear muffin-tin orbital method) and MAPW (modified augmented plane wave) methods [6, 7]. Svanidze and Morosan found evidence of Type I superconductivity in $ScGa_3$ and $LuGa_3$ single crystals. They measured the field and temperature dependent magnetization of the crystals [8]. The elastic, optical and thermodynamical properties of $ScGa_3$ and $LuGa_3$ were studied by FP-LAPW method by using the PBE-GGA and TB-mBJ schemes [9]. Heavy fermion superconductors $CePd_2Si_2$ and $CeIn_3$ were studied to understand the process of magnetically mediated superconductivity [10]. Normal-state properties of related structures such as YIn_3 have been also been measured by dHvA experiments. Measurement of resistivity, susceptibility and specific heats were made by Johnson et al. to study the superconducting transition in YIn_3 single crystals [11]. Thus it was observed that various materials with the $AuCu_3$ structure possess superconducting properties, amongst these $ScGa_3$ is known to exhibit very interesting properties. Similar to the filamentary superconductivity in YIn_3, it is proposed that the compound $ScIn_3$ may also possess similar superconducting properties.

In the present work, we have calculated electronic structure and transport properties of ScX_3 (X=Ga, In). To study the possible superconductivity in $ScIn_3$, we have compared the transport properties and extracted the Sommerfeld electronic component of specific heat γ. We have also computed the vibrational frequencies to study the nature of instabilities in these compounds.

The paper is organized as follows. Section II describes the computational methodology. The results and discussion are discussed in Section III. Finally, Section IV presents conclusion.

ISSN(Online): 2319-8753
ISSN (Print): 2347-6710

International Journal of Innovative Research in Science, Engineering and Technology

(A High Impact Factor, Monthly Peer Reviewed Journal)

Vol. 5, Issue 1, Januray 2016

II. MATERIALS & METHODS

In this paper, two computational methods within the density functional theory (DFT) were used in a complementary manner. For calculating the ground state electronic properties, we have adopted the method of full potential linearized augmented plane waves and local orbitals (lo) (Wien2K code) [12]. For the calculations we have used the generalized gradient approximation (GGA) to the exchange-correlation energy proposed by Wu and Cohen. The self-consistent energy and charge distributions were calculated numerically and the electronic and optical properties were derived from the converged configuration. The $R_{MT}K_{max}$ was set equal to 7 for the convergence parameter for which the calculation stabilizes and energy convergence was achieved. Here R_{MT} is the smallest muffin-tin radius and K_{max} is the cut-off wave vector of the plane-wave. The maximum radial expansion l_{max} was set to be 10. A mesh with 35 and 56 k-points for $ScGa_3$ and $ScIn_3$ was used in the IBZ. The energy cut-off between the core and valence states was set at −6.0 Ry.
The Vienna *ab initio* simulation package (VASP) [13], has been used to perform the structure optimization and to evaluate the Hellman-Feynmann forces. The projector augmented wave formalism implemented in this package gives very accurate results. The electronic exchange and correlations were treated by using the generalized gradient approximation (GGA) of Perdew, Burke and Ernzerhof (PBE). The 3d electrons of Sc and 4p/5p electrons of Ga/In have been included as valence electrons. The electronic wave functions were expanded in a plane wave basis with a cut-off of 250.925 eV and fine FFT grid was chosen with spacing around 0.5 A. The Brillioun zone sampling was done with a Monkhorst-Pack **k**-point grid of 4×4×4 for $ScGa_3$ and 3×3×3 for $ScIn_3$. The Fermi surface was treated by the Methfessel–Paxton method with a smearing of 0.2 eV. The vibrational free energy was obtained by using the phonon software (PHONON) [14] which uses the force constants provided by VASP. Phonon calculations were performed by the super cell approach. The calculations explore the full BZ and accounts for an interaction range of 10.0 Å, with asymmetric atoms displayed by +/- 0.02 Å. The optimized lattice parameters, pressure, volume etc. along with parameters such as Fermi energy are given in Table 1.

III. RESULTS & DISCUSSION

Crystal structure

The experimental lattice constant a=4.095 [8] for $ScGa_3$ was used for optimizing the lattice parameter by minimizing the ratio of the total energy of the crystal to its volume (volume optimization). The theoretical lattice constant a=4.09 Å was obtained corresponding to minimum volume of 461.75 $a.u^3$.

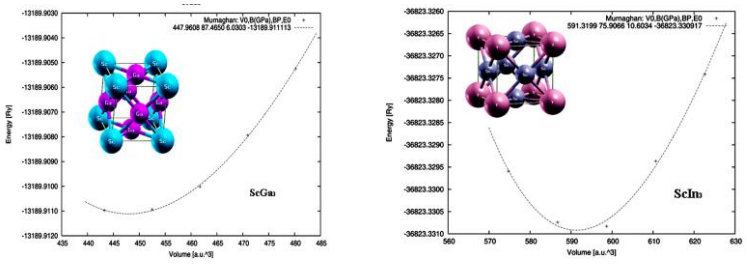

Figure 1. Dependence of total energy of cubic ScX_3(X=Ga, In) crystal on unit cell volume

The Sc atoms are positioned at (0, 0, 0) and Ga/In are positioned at (1/2, 1/2, 0). For the $ScGa_3$ and $ScIn_3$, the R_{MT} values are taken to be 2.50 Å for S, Ga and In atoms. Our ground state calculated parameters are listed in Table 1. The fitted curve for the Birch-Murnaghan's equation shows the total energy w.r.t volume of the unit cell after optimization of cubic states of ScX_3 (X=Ga, In) in Fig.1 (a, b). The crystal structures of $ScGa_3$ and $ScIn_3$ are shown in the inset.

The total energy of convergence and volume increases with changing cation and has a value of -13189.911 Ry for $ScGa_3$ and -36823.33 Ry for $ScIn_3$. The corresponding positive pressure of 87.46 and 75.9 GPa causes expansion during full geometry optimization. There is a 26% change in the volume of unit cell of $ScIn_3$ compared to $ScGa_3$, this causes ~9 % change in the Sc-Sc, Sc-X and X-X bond lengths. The bond lengths follow the trend Sc-Ga< Sc-In and In-In< Ga-Ga, which is due to increase in ion-size while going down the group. The systematic changes in the bond lengths are responsible for modifications in the band structure.

ISSN(Online): 2319-8753
ISSN (Print): 2347-6710

International Journal of Innovative Research in Science, Engineering and Technology

(A High Impact Factor, Monthly Peer Reviewed Journal)

Vol. 5, Issue 1, Januray 2016

The formation energies obtained from the calculations based on PAW method are -191.89 and -122.69 kJ/mol for $ScGa_3$ and $ScIn_3$ respectively. The negative sign indicates that the reaction is exothermic which implies stability of cubic binary intermettalic compounds.

Table 1. Input parameters FP-LAPW method

PROPERTIES		**$ScGa_3$**	**$ScIn_3$**
Space group & Lattice parameters (Å)	Calculated	Pm3m(221) a= 4.090	Pm3m(221) a=4.533
	Expt.	4.095 [**8**]	
R_{MT} (Å)		Sc=2.5 Ga=2.5	Sc=2.5 In=2.5
Bond length (Å)		Sc-Sc=4.09 Sc-Ga=2.89 Ga-Ga=2.89	Sc-Sc=4.46 Sc-In=3.15 In-In=3.15
Volume ($a.u^3$)		461.75	598.68
Pressure(GPa)		87.46	75.90
Formation energy(KJ/mol)		-191.89	-122.69
Transport properties	ρ (Ωm)	1.33×10^{-7}	1.93×10^{-7}
	k (W/K)	58.1	38.9
	S (V/K)	4.32×10^{-7}	1.22×10^{-5}
	R_H (m^3/C)	-1.67×10^{-10}	-4.31×10^{-10}
	γ(mJ/mol K^2)	5.40 7.03 [**8**]	3.73
	From DOS curve $N(\varepsilon_f)$	1.44	1.61
	Cal.T_C (K)	2.8 2.1 [**8**]	

Band structure and Density of States

The calculated band structures for RX_3 along the high-symmetry lines of Brillouin-zone (BZ) calculated by FPLAPW method are shown in Figs. 2. The band profiles are quite similar (with slight differences) and the metallic property of $ScGa_3$ and $ScIn_3$ is confirmed from their band structures. The major difference in the band dispersion is seen in the bands in the vicinity of Fermi level. In the valence band (VB), the bands which occur between -6.0 to -3.5 eV in $ScGa_3$ shift to higher energies between -5.0 to -2.5 eV in $ScIn_3$. A similar shift of bands occurs in the conduction band (CB), the bands between 2.5 and 4 eV shift to lower energies between 1.5 to 3 eV.

The minor differences in the band structures give rise to slight differences in the Fermi surfaces of $ScGa_3$ and $ScIn_3$. In both the compounds, the electron and hole pockets in the ΓM and XM directions give rise to complicated Fermi surface topologies. Hollow tube like structures are also observed along Γ-X directions. The size of the electron and hole pockets is found to decrease for $ScIn_3$ compared to $ScGa_3$, which may influence the superconducting property. The Fermi surfaces for $ScGa_3$ and $ScIn_3$ are shown (these were drawn using the XCrysden code) in the inset in Figs. 2. The geometry of the Fermi surface was characterized by Pluzhnikov et al. [6] by using the de Haas-van Alphen effect (dHvA) on single crystals of $ErGa_3$. A direct comparison is difficult to make but the obtained topology seems to indicate similarity with $ScGa_3$. The common features with $ErGa_3$ show that the Fermi surface sheets are complicated multiply conn ected hole centred around Γ and X points as observed from our calculations also.

ISSN(Online): 2319-8753
ISSN (Print): 2347-6710

International Journal of Innovative Research in Science, Engineering and Technology

(A High Impact Factor, Monthly Peer Reviewed Journal)

Vol. 5, Issue 1, January 2016

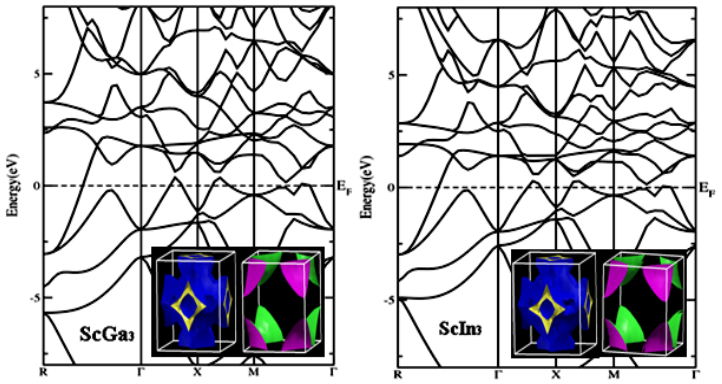

Fig. 2(a, b). Calculated high symmetry band structure of ScX_3(X=Ga, In)

The energy bands can be explained by plotting the total and partial electronic density of states (DOS) for the two compounds as shown in Figs. 3(a, b). The DOS are constructed for energy values between -10.0 to +10.0 eV and the key features such as the peaks and valleys for the two compounds are quite similar. In both the compounds the narrow bands between 0.5 and 2.0 eV above E_F are composed mainly of Sc d-states. The Fermi level is found to lie on a peak and is composed of Sc d-states which are hybridized with Ga/In s and p-states. Below E_F the Ga/In p-states dominate the VB, thereafter for lower energies beyond -4.0 eV, the main contributions are from s-states of Ga/In.

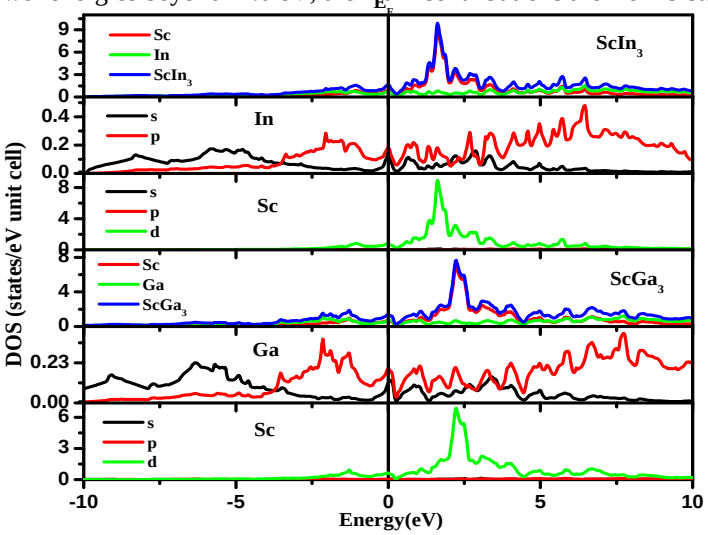

Fig. 3: Total and partial density of states of ScX_3(X=Ga, In)

The total density of states $N(E_F)$ increases from 1.44 states in $ScGa_3$ to 1.61 states/eV unit cell in $ScIn_3$ which is due to larger weight of Sc d-states at E_F in $ScIn_3$ compared to $ScGa_3$. The observed difference in states at the Fermi level are probably caused by the increase in environmental potential resulting from greater amount of charge transfer from Sc atom to the neighbouring In atoms in $ScIn_3$ compared to Sc to Ga atoms. Our computed values of $N(E_f)$ are underestimated compared to values of Svanidza and Morosan [8].

Charge density contour Plot

To understand the differences observed in the band topologies, the nature of the bonding in the compounds have been investigated. The distribution of bonding charge density in the (1 1 1) plane of $ScGa_3$ and $ScIn_3$ is shown in Figs. 4. It is observed that the charge density distribution around both Sc and Ga/In atoms are spherical-like. There is almost no

ISSN(Online): 2319-8753
ISSN (Print): 2347-6710

International Journal of Innovative Research in Science, Engineering and Technology

(A High Impact Factor, Monthly Peer Reviewed Journal)

Vol. 5, Issue 1, Januray 2016

overlapping electron distribution between Sc and Ga atoms, indicating an ionic bonding nature, whereas in the case of $ScIn_3$, there appears to be greater accumulation of charge. The differences in the various properties are therefore due to difference in the nature of bonding.

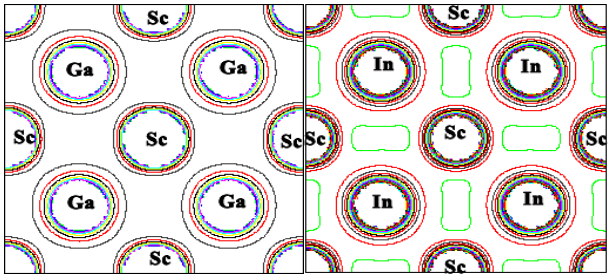

Fig. 4: Charge density distribution of ScX_3 along (111) plane in 2-D representation.

Optical properties

The optical properties may be derived from the knowledge of the complex dielectric function $\varepsilon(\omega) = \varepsilon_1(\omega)+i\varepsilon_2(\omega)$. The imaginary part $\varepsilon_2(\omega)$ is obtained from the momentum matrix elements between the occupied and unoccupied wave functions, whereas the real part $\varepsilon_1(\omega)$ of dielectric function can be derived from the imaginary dielectric function using the Kramers–Kronig relation.

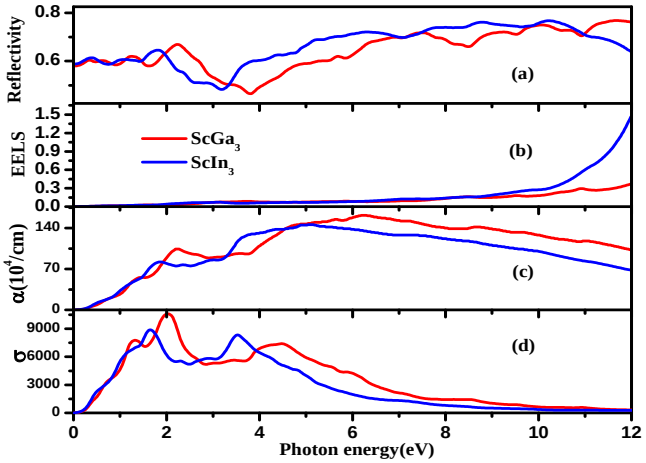

Fig. 5: Calculated optical properties of ScX_3(X=Ga, In)

The calculated optical properties at ground state for the energy range up to 12 eV are presented in Figs. 5. Due to the cubic nature of these compounds, only one dielectric tensor component is required to study the linear optical properties. The origin of the peaks in the real and imaginary parts of the dielectric functions are attributed to the interband transition from occupied to unoccupied states. It is seen that the optical spectrum of $ScGa_3$ and $ScIn_3$ differ owing to the different band structures and different peak positions in the density of states (Figs. 2 and 3).

From the imaginary part of dielectric function $\varepsilon_2(\omega)$, it is observed that the optical transitions begin at 0.70 eV for $ScGa_3$ and at 0.5 eV for $ScIn_3$ (not shown here). The highest peaks are located at 1.22 eV and 1.05 eV in the IR regions corresponding to $ScGa_3$ and $ScIn_3$ respectively. Absorption rapidly falls to very low values beyond 8.3 eV in both the cases. From the real part $\varepsilon_1(\omega)$ which are obtained from $\varepsilon_2(\omega)$ using the Kramers-Kronig conversion, it is observed that in the zero frequency limit the value of $\varepsilon_1(0)$ is 54.32 and 57.25 for $ScGa_3$ and $ScIn_3$ respectively. The dielectric function goes to zero at 2.00 and 1.6 eV for $ScGa_3$ and $ScIn_3$ respectively, beyond which the values of $\varepsilon_1(\omega)$ become

ISSN(Online): 2319-8753
ISSN (Print): 2347-6710

International Journal of Innovative Research in Science, Engineering and Technology

(A High Impact Factor, Monthly Peer Reviewed Journal)

Vol. 5, Issue 1, Januray 2016

negative. Similarly, the static refractive index n(0) is found to have the value 7.36 and 7.57 corresponding to $ScGa_3$ and $ScIn_3$ respectively.

The optical conductivity of $ScGa_3$ and $ScIn_3$ are plotted as a function of photon energy. Since the intermetallics have no band gap as is evident from the band structures, the photoconductivity starts with zero photon energy for each of the phases. These spectra have several maxima and minima within the energy range studied. The photo conductivities and hence optical conductivities of the materials increases as a result of absorbing photons and falls to low values beyond 11 eV in UV regions. The optical conductivity increases rapidly in $ScGa_3$ and shows a narrow peak at 1.3 eV which is followed by the highest peak with a value of 10650 $(\Omega cm)^{-1}$ at 2.06 eV in visible region. Maximum conductivity is obtained in $ScIn_3$ at 1.63 eV with σ=8959 $(\Omega cm)^{-1}$. Similarly, the absorption coefficient spectra show peaks at 1.8 and 3.68 eV for $ScIn_3$, whereas the peak occurs at 2.21 eV in $ScGa_3$. Reflectivity at zero photon energy for $ScGa_3$ is 57 %, which increases marginally to 66 % at 2.25 eV. In $ScIn_3$, the reflectance is 58% which increases to 64 % at 1.8 eV. Reflectance drops to 45 % beyond 3.2 eV in the ultraviolet region. Both $ScGa_3$ and $ScIn_3$ can therefore have applications as possible shields for ultraviolet radiations.

Phonon spectra and thermodynamic property:

We perform the phonon calculations by the PAW method in order to study the stability of ScX_3 compounds, and to understand the nature of superconductivity. The phonon spectra of $ScGa_3$ are calculated by using 4×4×4 super cell and $ScIn_3$ are calculated by using 3×3×3 super cell along the high symmetry directions R-X-Γ-M-R-Γ of the BZ as shown in Figs. 6 (a, b). It is observed that there is a strong dispersion of phonon modes in $ScGa_3$ starting from 3.2 THz at the X-point which converges at 0.068i THz at the zone center. In the case of $ScIn_3$, the dispersion begins at ~2 THz and converges at 0.152 THz at the G-point. The branch along the G-M direction shows pronounced anomaly in $ScGa_3$ which are also seen in the band structure in Fig. 2a. Such softening of mode is not observed in $ScIn_3$.
From the PDOS of each displaced atom (not shown here) and the polarization vector analysis, it is found that phonon modes between 0 and 4 THz are essentially dominated by the motion of heavy Ga atoms while the Sc atoms give lower contribution to these phonon modes. The phonon modes between 5 to 7 THz are essentially dominated by the Sc atoms. It is seen that the low energy infrared (IR) vibrations which are dominated by both Sc-Ga atoms, exhibit instability and the characteristic frequency is imaginary. In the case of $ScIn_3$, the vibrational modes between 0 to 3.5 THz are predominantly due to In atoms and the high frequency modes between 3.5 to 5 THz are contributed by Sc atoms. Stronger bonding in the case of $ScGa_3$ also gives rise to higher vibrational frequencies as can be observed from the IR modes given in Table 2. Thus, both the electronic and lattice dispersions show similar nature, from which it can be inferred that the phonon modes are strongly coupled to the electronic system in the case of $ScGa_3$ giving rise to softening of vibrational modes, In absence of imaginary vibrational modes $ScIn_3$ appears to be a more stable intermetallic, which suggests occurrence of superconductivity.

Transport properties

Superconductivity in $ScGa_3$ has been investigated by exploring the electrical resistivity, magnetic susceptibility and specific heats down to 0.4 K [8]. Although experimental studies for $ScIn_3$ are not available in literature, similarities in the electronic structure of $ScGa_3$ and $ScIn_3$ suggest that $ScIn_3$ may also display ground state superconductivity. To understand the superconducting nature in these alloys, the transport properties are calculated [15]. Temperature dependent properties have been plotted in Fig. 7.

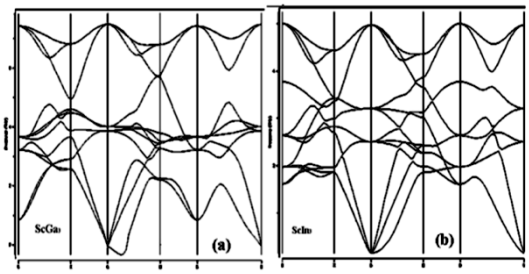

Fig. 6: Phonon dispersion curves of ScX_3

ISSN(Online): 2319-8753
ISSN (Print): 2347-6710

International Journal of Innovative Research in Science, Engineering and Technology

(A High Impact Factor, Monthly Peer Reviewed Journal)

Vol. 5, Issue 1, Januray 2016

Table 2: Vibrational modes of ScX_3

$ScGa_3$		$ScIn_3$	
Modes	cm^{-1}	Modes	cm^{-1}
$T_{1u}(I)$	2.3i	$T_{1u}(I)$	5.1
$T_{1u}(I)$	128.8	$T_{1u}(I)$	83.5
T_{2u}	133.9	T_{2u}	107
$T_{1u}(I)$	249.6	$T_{1u}(I)$	166

The electrical conductivity of the ScX_3 compounds is of the order ~10^6 $(\Omega m)^{-1}$ at room temperature. At low temperatures <100 K, the electrical resistivity of $ScGa_3$ is found to increase rapidly to a value of 0.7×10^{-6} Ωm. Similarly, the thermal conductivity of $ScGa_3$ and $ScIn_3$ show the same values at low temperatures (<50 K) and rises rapidly with increasing temperature in $ScGa_3$ compared to $ScIn_3$. At ambient temperatures the Seebeck coefficient for $ScIn_3$ is higher (12.2 μV/K) than $ScGa_3$, the Hall coefficient also shows similar temperature dependence. From the –ve sign of the Hall coefficient we can infer that the major charge carriers are electrons in both the intermetallics. The no. of charge carriers in $ScGa_3$ and $ScIn_3$ are 3.9×10^{22} and 1.4×10^{22} cm^{-3} respectively.

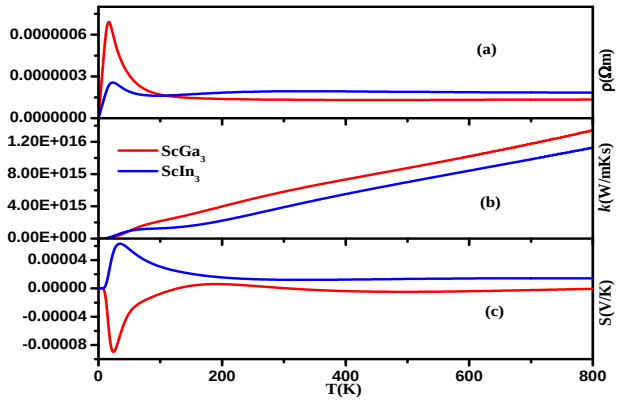

Fig. 7: Transport properties of ScX_3(X=Ga, In) (a) Resistivity (b) Thermal conductivity (c) Seebeck coefficient

The specific heats of both the intermetallics are nearly the same in the entire temperature range although $ScGa_3$ has a marginally higher value compared to $ScIn_3$. By fitting the measured specific heat at low temperature to the relation $C_P = \gamma T + \beta T^3$, the electronic specific heat coefficient γ of RX_3 can be obtained. From Table 1, the values of γ are 5.4 and 3.73 mJ/molK^2 corresponding to $ScGa_3$ and $ScIn_3$ respectively. The value of the average electron-phonon coupling constant λ_{ep} may be estimated from the relation $\gamma^{exp}/\gamma^{calc}=1+\lambda_{ep}$. The experimental value of γ (7.1 mJ/mol K^2) for $ScGa_3$ [10] are larger than that obtained by FP-LAPW and PP methods. From the above relation the calculated value of λ_{ep} is 0.31, which is lower compared to previous calculations. This may be due to well the known problem of underestimation of eigenvalues in the DFT method which causes the transport properties to be underestimated compared to experiment. The value of λ_{ep}=0.31 implies that $ScGa_3$ is an intermediate coupling superconductor. Experimental values of γ for $ScIn_3$ are not available for comparison.

The superconductivity transition temperature for $ScGa_3$ may be calculated using the McMillan formula.

$$T_c = \frac{\theta_D}{1.45}\exp\left\{-\frac{1.04(1+\lambda)}{\lambda-\mu^*(1+0.62\lambda)}\right\}$$

Using a typical value of μ*=0.13, which represents the repulsive screened coulomb potential and the Debye temperature θ_D=660 K [10] leads to a calculated value of T_c=2.8 K. This value of transition temperature is in excellent agreement with the experimental value of 2.1 K, given the uncertainty of the parameters of the McMillan's formula.

ISSN(Online): 2319-8753
ISSN (Print): 2347-6710

International Journal of Innovative Research in Science, Engineering and Technology

(A High Impact Factor, Monthly Peer Reviewed Journal)

Vol. 5, Issue 1, Januray 2016

IV. CONCLUSION

The FPLAPW-GGA and VASP methods have been used for study of the electronic and vibrational properties of newly discovered 2.1 K superconductor $ScGa_3$ as well as its isostructural alloy $ScIn_3$. We found that the main contributions to the density of states at the Fermi level come from the Sc *d*-states and Ga/In-p states. From the calculated specific heats, the electron-phonon coupling constant $\lambda_{el\text{-}ph}$ has a value of 0.31 and yields a T_c of 2.8 K for $ScGa_3$. The coupling leads to phonon instability only in $ScGa_3$ as observed from the phonon dispersion modes. The electronic and lattice dispersions of $ScGa_3$ and $ScIn_3$ show very similar nature, and the optical and transport properties are marginally different. These observations suggest the occurrence of superconductivity in $ScIn_3$. Vibrational spectra measurements are required to verify the calculations.

ACKNOWLEDGMENTS

We wish to thank Prof. P. Blaha and his team for the WIEN2k code and Prof. Hafner for the VASP code.

REFERENCES

[1] Havinga, E. E., Damsma, H., and Van Maaren, M.H., "Oscillatory dependence of electronic properties of alloys with Cu_3Au-type structure; band structure calculations" J. Phys. Chem. Solids Vol.31, pp.2653, 1970.
[2] Bittar, E. M., Adriano, C., Giles, C., Rettori, C., Fisk, Z., and Pagliuso, P.G., "Electron spin resonance study of the $LaIn_{3-x}Sn_x$ superconducting system" J. Phys. Condens. Matter Vol.23, pp.455701, 2011.
[3] Ram, S., Kanchana, V., Vaitheeswaran, G., Svane, A., Dugdale, S. B., and Christensen, N. E., "Electronic topological transition in $LaSn_3$ under pressure" Phys. Rev. B Vol.85, pp.174531, 2012.
[4] Dugdale, S. B., "First-principles study of electron-phonon superconductivity in YSn_3" Phys. Rev. B Vol.83, pp.012502, 2011.
[5] Ram, S., Kanchana, V., Svane, A., Dugdale, S. B., and Christensen, N. E., "Fermi surface properties of AB_3 (A = Y, La; B = Pb, In, Tl) intermetallic compounds under pressure" J. Phys.: Condens. Matter Vol.25, pp.155501, 2013.
[6] Pluzhnikov, V.B., Czopnik, A., Svechkarev, I.V., "de Haas-van Alphen effect in $ScGa_3$, $LuGa_3$ and YIn_3'' Physica B Vol. 212, pp.375, 1995.
[7] Bross, H., and Eder, R., "Self-consistent MAPW calculation with a warped muffin-tin potential. I. The electronic structure of Al and its pressure dependence," Physica Status Solidi B, vol. 144, no. 1, pp. 175–193, 1987.
[8] Svanidze, E., and Morosan, E., "Type-I superconductivity in $ScGa_3$ and $LuGa_3$ single crystals" Phys. Rev. B, Vol. 85, pp.174514, 2012.
[9] Murtaza, G.,Gupta, S. K., Seddik, T., Khenata, R., Alahmed, Z. A., Ahmed, R., Khachai, H., Jha, P. K., Bin Omran, S.,"Structural, electronic, optical and thermodynamic properties of cubic $REGa_3$ (RE=Sc or Lu) compounds: Ab initio study" Journal of Alloys and Compounds,Vol.597,pp.36-44,2014.
[10] Johnson, S. D., Young, J. R., Zieve, R. J., Cooley, J. C., "Superconductivity in single-crystal YIn_3'' Solid State Communications Vol.152, pp.513-515, 2012.
[11] Mathur, N. D., Grosche, F. M., Julian, S. R., Walker, I. R., Freye, D. M., Haselwimmer, R. K. W, and Lonzarich, G. G.,"Magnetically mediated superconductivity in heavy fermion compounds" Nature, Vol.394, pp. 39,1998.
[12] Blaha, P., Schwarz, K., Madsen, G.K.H., Kuasnicka D.J., & Luitz, WIEN2K, An Augmented Plane Waveve+ Local Orbitals Program for Calculating Crystal Properties. (2001). K. Schwarz Technical Universitat, Wien, Austria, ISBN 3-9501031-1-2.
[13] Kresse, G., Hafner, J., "ab-intio molecular dynamics for open shell transition metals"Phys. Rev. B. Vol.48, pp. 13115. 1993.
[14] Parlinski, K., Li, Z. Q., and Kawazoe, Y., "First principles determination of the soft mode in cubic ZrO_2," Phys. Rev. Lett. Vol.78, pp.4063-4072, 1997.
[15] Madsen G. K. H., and Singh, D. J., "A BoltzTrap: code for calculating band structure dependent quantities"Comput. Phys. Commun., Vol.175 pp.67-71, 2006.